DETECTION OF COHERENT BEAM-BEAM MODES WITH DIGITIZED BEAM POSITION MONITOR SIGNALS

G. Stancari* and A. Valishev, Fermi National Accelerator Laboratory, Batavia, IL 60510, USA
S. M. White, Brookhaven National Laboratory, Upton, NY 11973, USA

Abstract

A system for bunch-by-bunch detection of transverse proton and antiproton coherent oscillations in the Fermilab Tevatron collider is described. It is based on the signal from a single beam-position monitor located in a region of the ring with large amplitude functions. The signal is digitized over a large number of turns and Fourier-analyzed offline with a dedicated algorithm. To enhance the signal, band-limited noise is applied to the beam for about 1 s. This excitation does not adversely affect the circulating beams even at high luminosities. The device has a response time of a few seconds, a frequency resolution of 1.6×10^{-5} in fractional tune, and it is sensitive to oscillation amplitudes of 60 nm. It complements Schottky detectors as a diagnostic tool for tunes, tune spreads, and beam-beam effects. Measurements of coherent mode spectra are presented and compared with models of beam-beam oscillations.

INTRODUCTION

In particle colliders, each beam experiences nonlinear forces when colliding with the opposing beam. A manifestation of these forces is a vibration of the bunch centroids around the closed orbit. These coherent beam-beam oscillation modes were observed in several lepton machines, including PETRA, TRISTAN, LEP, and VEPP-2M [1, 2, 3, 4]. Although their observation in hadron machines is made more challenging by the lack of strong damping mechanisms to counter external excitations, they were seen at the ISR, at RHIC, in the Tevatron, and in the LHC [5, 6, 7, 8, 9, 10, 11]. Originally, one motivation for the study of coherent beam-beam modes was the realization that their frequencies may lie outside the incoherent tune distribution, with a consequent loss of Landau damping [12]. The goal of the present research is to develop a diagnostic tool to estimate bunch-by-bunch tune distributions, to assess the effects of Gaussian electron lenses for beam-beam compensation [13, 14, 15, 16], and to provide an experimental basis for the development of beam-beam numerical codes.

The behavior of colliding bunches is analogous to that of a system of oscillators coupled by the beam-beam force. In the simplest case, when 2 identical bunches collide head-on in one interaction region, 2 normal modes appear: a σ mode (or 0 mode) at the lattice tune, in which bunches oscillate transversely in phase, and a π mode, separated from the σ mode by a shift of the order of the beam-beam parameter, in which bunches are out of phase. In general, the number, frequency, and amplitude of these modes depend on the number of bunches, on the collision pattern, on the tune separation between the two beams, on transverse beam sizes, and on relative intensities. Coherent beam-beam modes have been studied at several levels of refinement, from analytical linear models to fully 3-dimensional particle-in-cell calculations [1, 9, 17, 18, 19, 20, 21, 22, 23, 24].

In the Tevatron, 36 proton bunches (identified as P1–P36) collided with 36 antiproton bunches (A1–A36) at the center-of-momentum energy of 1.96 TeV. There were 2 head-on interaction points (IPs), corresponding to the CDF and the DZero experiments. Each particle species was arranged in 3 trains of 12 bunches each, circulating at a revolution frequency of 47.7 kHz. The bunch spacing within a train was 396 ns, or 21 53-MHz rf buckets. The bunch trains were separated by 2.6-μs abort gaps. The synchrotron frequency was 34 Hz, or 7×10^{-4} times the revolution frequency. The machine operated with betatron tunes near 20.58.

The betatron tunes and tune spreads of individual bunches are among the main factors that determine beam lifetimes and collider performance. They are affected by head-on and long-range beam-beam interactions. Three systems were used in the Tevatron to measure incoherent tune distributions: the 21.4-MHz Schottky detectors, the 1.7-GHz Schottky detectors, and the direct diode detection base band tune (3D-BBQ). The latter two could be gated on single bunches. Detection of transverse coherent modes complemented these three systems because of its sensitivity, bunch-by-bunch capability, high frequency resolution, and fast measurement time.

The basis for the measurement technique was presented in Ref. [25], and preliminary results can be found in Refs. [26, 27, 28]. Several improvements, mainly in the data analysis, were implemented and presented in a concise report [29]. A comprehensive description of the technique and of observations in a wide range of experimental conditions was reported in Ref. [10]. Here, we focus on the detection of coherent beam-beam oscillations and on comparisons with analytical and numerical models.

MODELS

In the Tevatron, transverse coherent oscillations were substantially nonlinear due to the properties of the lattice and of the beam-beam force. We first used the rigid-bunch approximation for a fast analysis of the expected beam-beam mode frequencies and their dependence on the the

* E-mail: stancari@fnal.gov.

betatron tunes Q and on the beam-beam parameter per interaction point ξ. For a more accurate description of the coherent mode spectrum, tracking simulations with a strong-strong 3-dimensional numerical code were employed.

We used a simple matrix formalism to compute the eigenmode tunes of the system of colliding bunches. Besides employing the rigid bunch approximation, one more simplification was used. The complete description of the system would require modeling the interaction of 72 bunches at 138 collision points. The analysis of such a system can be quite complex. Observations and analytical estimates showed that the difference in tunes between individual bunches was small compared to the beam-beam tune shift. Thus, as a first approximation, it is possible to neglect long-range interactions. This reduces the system to 6 bunches (3 in each beam) colliding at two head-on interaction points. In the following discussion, we restrict betatron oscillations to one degree of freedom. Because the system has 3-fold symmetry, the 1-turn map transporting the 12-vector of dipole moments and momenta of the system of 6 bunches can be expressed as follows:

$$M = M_{\mathrm{BB3}}\, M_{\mathrm{T3}}\, M_{\mathrm{BB2}}\, M_{\mathrm{T2}}\, M_{\mathrm{BB1}}\, M_{\mathrm{T1}}, \qquad (1)$$

where M_{TN} ($N = 1,2,3$) are the 2×2 block-diagonal, 12×12 matrices transporting phase space coordinates through the accelerator arcs, and M_{BBN} are the matrices describing thin beam-beam kicks at the IPs. Although there are only 2 interactions per bunch, 3 collision matrices are used to describe a one-turn map of the system of 6 bunches. This construction represents the time propagation of the bunch coordinates through one turn with break points at the CDF (B0), D0 and F0 locations in the machine. If on a given step the bunch is at B0 or D0, its momentum coordinate is kicked according to the distance between the centroids of this bunch and of the opposing bunch. If the bunch is at F0 (1/3 of the circumference from B0 and D0), where the beams are separated, its momentum is unchanged. The eigentunes of the 1-turn map can then be computed numerically. We will use the symbols ξ_p and ξ_a for the beam-beam parameters of protons and antiprotons; β is the amplitude

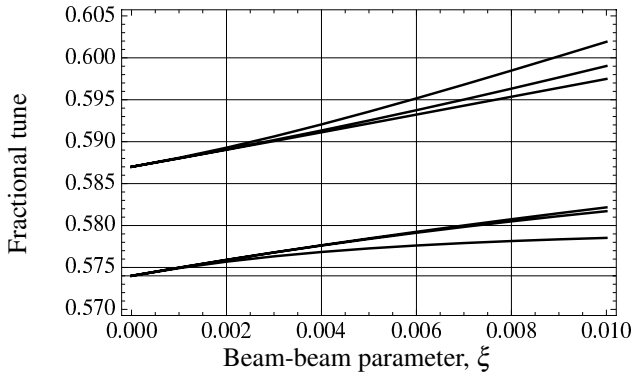

Figure 1: Coherent mode tunes vs. beam-beam parameter calculated with the linearized model; $Q_p = 0.587$, $Q_a = 0.574$, $\xi = \xi_p = \xi_a$.

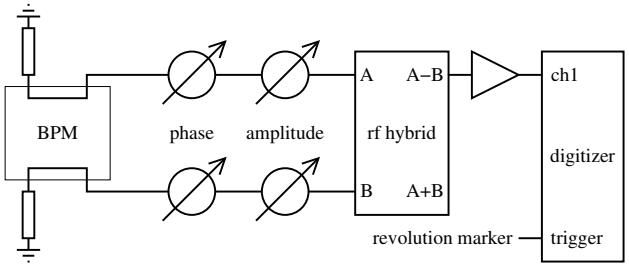

Figure 2: Schematic diagram of the apparatus.

function at the IP. The Yokoya factor [18, 30] is assumed to be equal to 1.

This model provides a quick estimate of the expected values of the coherent beam-beam mode tunes for a given set of machine and beam parameters. In Figure 1, an example of the dependence of the 6 eigenfrequencies on the beam-beam parameter per IP is presented. As one would expect, at small values of ξ (uncoupled oscillators) the mode frequencies approach the bare lattice tunes; in this case, 0.587 for protons and 0.574 for antiprotons. When the total beam-beam parameter exceeds the difference between the lattice tunes, the modes are split and their symmetry approaches that of the conventional σ and π modes. The parameters of this calculation are taken to resemble those of the beginning of the Tevatron Store 7754, when the beam-beam parameter was $\xi = \xi_a = \xi_p = 0.01$. A comparison with data is given in the results section (Figure 4).

A more complete description of coherent oscillations was provided by numerical simulations based on the code BeamBeam3D [22]. BeamBeam3D is a fully parallelized 3-dimensional code allowing for self-consistent field calculations of arbitrary distributions and tracking of multiple bunches. Transport from one IP to the other is done through linear transfer maps. The electromagnetic fields generated by the beams are calculated from the Poisson equation using a shifted Green-function method efficiently computed with a fast-Fourier-transform (FFT) algorithm on a uniform grid.

The measured beam intensities and emittances were used in the simulation. Lattice parameters were measured on the proton orbit. The bare lattice tunes were derived from the main quadrupole currents. Due to the asymmetry of the collision IPs in the Tevatron, the bunches coupled by groups of 3 through the head-on interactions. In the simulations, 3 bunches per beam were therefore tracked to reproduce the spectrum of centroid oscillations. A comparison between the calculated and measured spectra for the case of Tevatron Store 7754 is discussed in the results section and shown in Figure 4.

APPARATUS

The system for the detection of transverse coherent modes (Figure 2) was based on the signal from a single vertical beam-position monitor (BPM) located near the CDF interaction point, in a region where the vertical amplitude

function at collisions was $\beta_y = 880$ m. The BPM was a stripline pickup, with two plate outputs (A and B) for each of the two counterpropagating beams.

In the Tevatron, protons and antiprotons shared a common vacuum pipe. Outside of the interaction regions, their orbits wrapped around each other in a helical arrangement. Therefore, bunch centroids were several millimeters away from the BPM's electrical axis. Typically, the peak-to-peak amplitude of the proton signal was 10 V on one plate and 5 V on the other, whereas the signal of interest was of the order of a few millivolts. For this reason, it was necessary to equalize the A and B signals to take advantage of the full dynamic range of the digitizer. Equalization also reduced false transverse signals due to trigger jitter, as discussed below. The phase and attenuation of each signal was manually adjusted by minimizing the $A-B$ output of the rf hybrid circuit. If necessary, fine-tuning could be done by displacing the beam with a small orbit bump. Orbits at collisions were stable over a time scale of weeks, and this manual adjustment did not need to be repeated often.

The difference signal from the hybrid was amplified by 23 dB and sent to the digitizer. We used a 1-channel, 1-V full range, 10-bit digitizer with time-interleaved analog-to-digital converters (ADCs). It sampled at 8 gigasamples/s (GS/s) and stored a maximum of 1024 megasamples (MS) or 125,000 segments. (Due to a firmware problem, only half of the segments were used in the experiments described below.) The 47.7-kHz Tevatron revolution marker was used as trigger, so we refer to 'segments' or 'turns' interchangeably. Typically, we sampled at 8 GS/s (sample period of 125 ps), i.e. 150 slices for each 19-ns rf bucket. At this sampling rate, one could record waveforms of 1 bunch for 62,500 turns, 2 bunches for 52,707 turns, or 12 bunches for 12,382 turns, depending on the measurement of interest. A C++ program running on the front-end computer controlled the digitizer settings, including its delay with respect to the Tevatron revolution marker.

The recorded output data contained the raw ADC data together with the trigger time stamps and the delay of the first sample with respect to the trigger. Timing information had an accuracy of about 15 ps, and it was extremely important for the synchronization of samples from different turns.

To enhance the signal, the beam was excited with a few watts of band-limited noise ('tickling') for about 1 s during the measurement. The measurement cycle consisted of the following steps: digitizer setup, tickler turn-on, acquisition start, tickler turn-off, and acquisition stop. The cycle took a few seconds. The procedure was parasitical and it did not adversely affect the circulating beams, even at the beginning of regular collider stores, with luminosities around 3.5×10^{32} events/(cm^2 s). When repeating the procedure several times, the Schottky monitors occasionally showed some activity, but no beam loss was observed.

DATA ANALYSIS

Data was analyzed offline using the multi-platform, open-source R statistical package [31]. The distribution of differences between trigger time stamps from consecutive turns was used to obtain the average revolution frequency (47713.11 Hz at 980 GeV). From it, the nominal or 'ideal' trigger time stamps for each turn were calculated. The distribution of trigger offsets, i.e. the differences between measured and nominal time stamps, is a measure of the jitter in the revolution marker. The root mean square of the distribution was usually less than 0.2 ns. The delay between trigger time and the time stamp of the first sample was also recorded with an accuracy of 15 ps. The sum of trigger offset and first-sample delay is the correction by which each sample in a segment is to be shifted in time to be aligned with the other segments. For each turn and each bunch, the signal was interpolated with a natural spline and shifted in time according to this correction. One undesirable effect of this synchronization algorithm is that a few slices (usually not more than 3) at each edge of the bucket become unusable, as they cannot be replaced with real data. The synchronization of turns is extremely important, as the jitter in trigger time translates into a false transverse oscillation where the difference signal has a slope. If the BPM plates are not perfectly balanced, jitter of even a fraction of a nanosecond can raise the noise floor by several decibels and compromise the measurement.

Bunch oscillations were dominated by low-frequency beam jitter attributable to mechanical vibrations [32, 33]. The range of amplitudes was inferred from comparisons with the regular Tevatron BPM system and corresponds to about ±25 μm. This low-frequency jitter did not affect the measurements of coherent beam-beam modes directly, but it reduced the available dynamic range. A high-pass filter and more amplification may be used to improve the system.

For each bunch, the signal of each individual slice vs. turn number was Fourier transformed. Frequency resolution is determined by the number of bins in the FFT vector and it is limited to 62,500 turns, corresponding to 1.6×10^{-5} of the revolution frequency or 0.8 Hz. The data was multiplied by a Slepian window of rank 2 to confine leakage to adjacent frequency bins and suppress it below 10^{-5} in farther bins [34]. When the full frequency resolution was not needed, the FFT vectors were overlapped by about 1/3 of their length to reduce data loss from windowing, and the resulting spectral amplitudes were averaged. Calculations took about 20 s per bunch for 62,500 turns and 150 slices per bunch on a standard laptop computer. Processing time was dominated by the synchronization algorithm.

The noise level was estimated by observing the spectra without beam. The spectra showed a few sharp lines in all slices. These lines were attributed to gain and offset differences between the time-interleaved ADCs themselves and to timing skew of their clocks. To improve the signal-to-noise ratio, and to suppress backgrounds unrelated to the

beam such as the spurious lines from the digitizer, a set of signal slices (near the signal peaks) and a set of background slices (before the arrival of the bunch) were defined. Amplitude spectra were computed for both signal and background slice sets, and their ratio was calculated. The ratios are very clean, with some additional variance at the frequencies corresponding to the narrow noise spikes. Results are presented in terms of these signal-to-background amplitude ratios.

Figure 3 shows an example of analyzed antiproton data, in two regions of the frequency spectrum: a low-frequency region with the horizontal axis expressed in hertz (top two plots) and a high-frequency region, in terms of the revolution frequency or fractional tune. The 2-dimensional color plots show the amplitude distribution for each of the 150 125-ps slices in logarithmic scale. In this example, the signal slices are numbers 41–95 and 99–147. They are defined as the ones for which the amplitude is above 10% of the range of amplitudes. Background slices are numbers 3–31 (amplitude below 2% of range). The black-and-white 1-dimensional plots show the ratio between signal and background amplitudes. In the top plots of Figure 3, one can appreciate the strength of the low-frequency components. The 60-Hz power-line noise and its harmonics are also visible. The lines around 34 Hz and 68 Hz are due to synchrotron oscillations leaking into the transverse spectrum. The bottom plots of Figure 3 show the spectra of transverse coherent oscillations. The vertical lines present in all slices in the 2-dimensinal plot, attributed to digitizer noise, are eliminated by taking the ratio between signal and background slices. One can also notice the small variance of the noise level compared to the amplitude of the signal peaks.

In the 2-dimensional plots of Figure 3, one may notice patterns in the oscillation amplitude as a function of position along the bunch. These may be an artifact of the imperfect synchronization between the *A* and *B* signals, but they may also be related to the physical nature of the coherent modes (i.e., rigid vs. soft bunch, head-on vs. long range). The phase of the oscillations as a function of frequency and bunch number may also provide physical insight.

RESULTS

Transverse coherent mode spectra were measured for both proton and antiproton bunches under a wide range

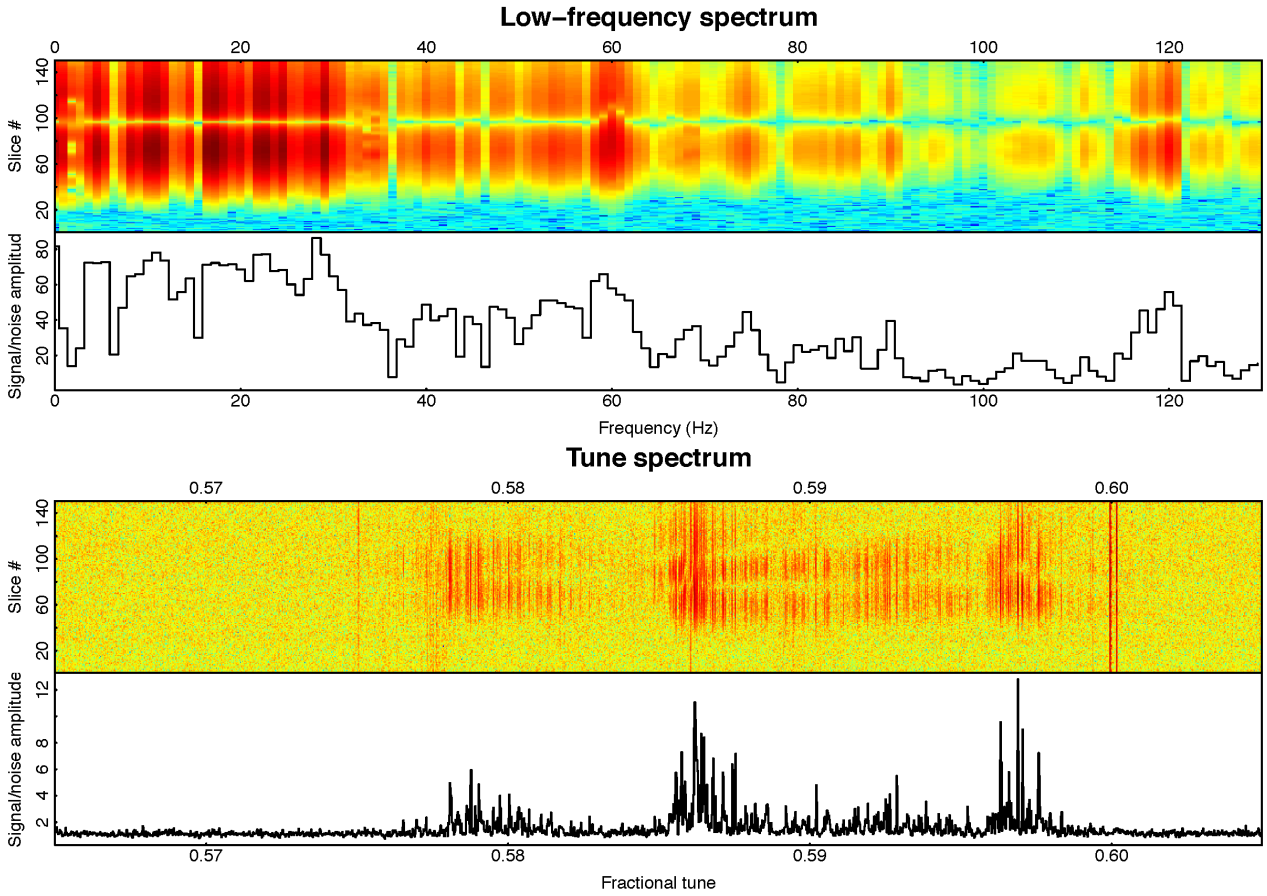

Figure 3: Example of frequency spectra for antiprotons from data taken during Store 7754. Two selected regions of the spectrum are shown: below 130 Hz (top two plots) and around $(47.7\ \text{kHz}) \times (1 - 0.585) = 20\ \text{kHz}$ (bottom two plots). The color plots represent the Fourier amplitude (in logarithmic scale) vs. frequency for each of the 150 125-ps slices. The black traces are the average amplitudes of the signal slices divided by those of the background slices.

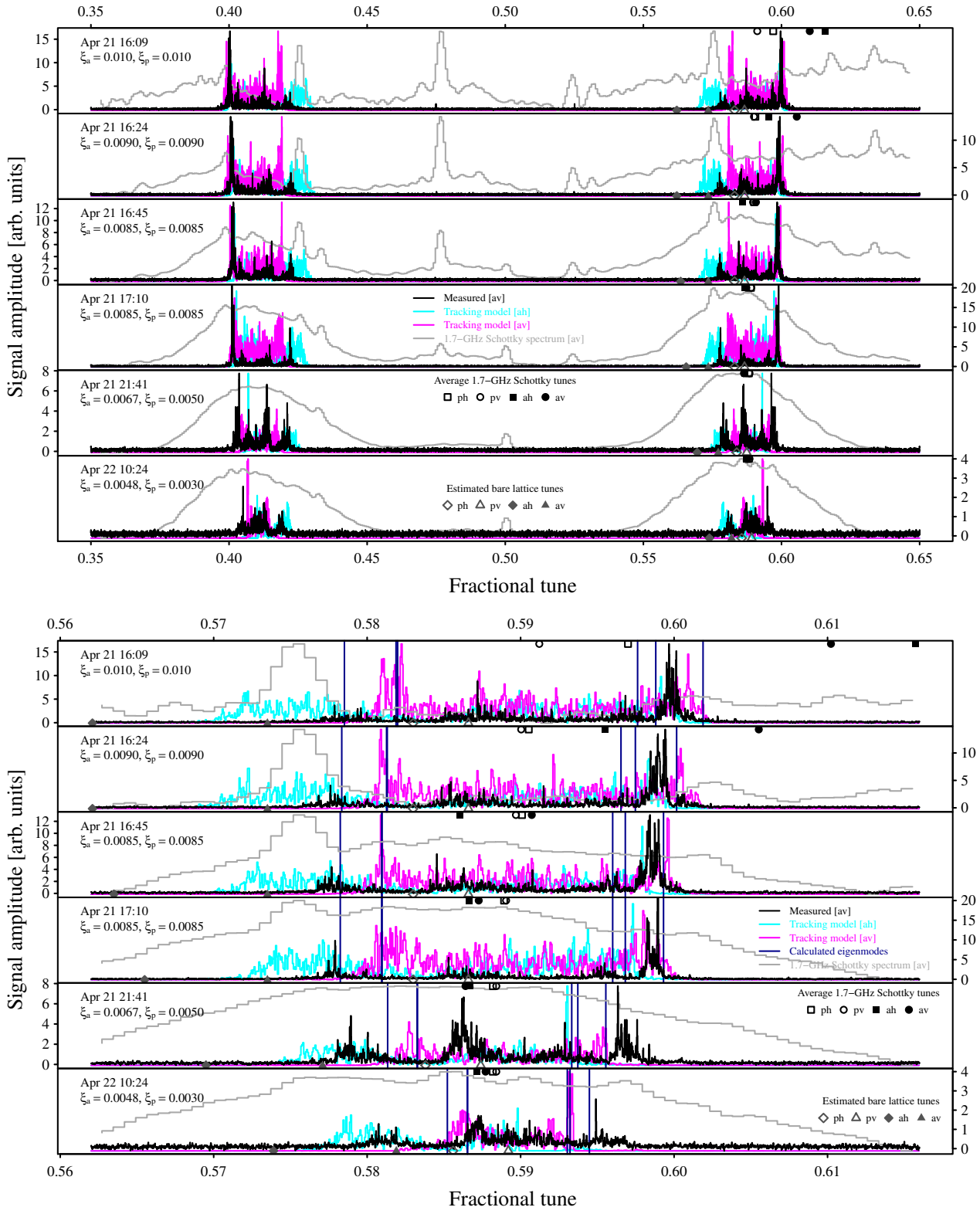

Figure 4: Evolution of vertical coherent beam-beam modes for antiproton bunch A13 during the course of Store 7754.

of experimental conditions [10]. In this section, we focus on the observation of coherent beam-beam modes, on their evolution over the course of a collider store, and on comparisons with analytical and numerical models.

An illustration of the evolution of transverse coherent modes during a collider store is shown in Figure 4 for vertical antiproton oscillations. The top plot covers a wide range of fractional tunes, while the bottom one shows the details near the betatron frequencies. The black line represents the measured spectra. The gray histogram shows the measured 1.7-GHz antiproton vertical Schottky spectra for comparison. The cyan and magenta lines are the antiproton horizontal (ah) and antiproton vertical (av) spectra calculated with the BeamBeam3D code. The bottom plot shows the 6 calculated rigid-bunch modes as vertical dark blue lines. Markers are used to indicate the average Schottky tunes (black) and the estimated bare lattice tunes (dark gray) for protons and antiprotons, both horizontally and vertically (ph, pv, ah, and av). The first 4 spectra were acquired within about 1 hour after the beams were brought in collision. The 5th plot was taken after about 6 hours, whereas the last plot was taken at the end of the store, just before the beams were dumped. The calculated beam-beam parameters per IP, ξ_a and ξ_p, are printed on the left side of each plot.

Over the course of a store, the lattice tunes need to be periodically adjusted to keep the average incoherent tune close to the desired working point. Except for the last two measurements, which may be affected by the evolving linear coupling and by a slight miscalibration of the tune settings, the estimated lattice tune (dark gray triangles) lies below the first group of eigenmodes, as expected.

One can clearly see how, as the beam-beam force weakens, the spread in coherent modes decreases, and so does the amplitude of the π mode (near 0.60). The asymmetries between the beams, the large number of bunches, and the multiple collision points give rise to a rich spectrum of oscillations.

A comparison with the Schottky spectra reveals many common coherent spikes. The ones at 0.475/0.525, visible in both the Schottky spectrum and in the digitized-BPM spectrum, are unexplained. Because of the distortions of the Schottky spectrum at the beginning of the store, the present system provides a better indication of the tune distribution under these conditions.

The predicted eigenfrequencies of the simplified rigid-bunch model are close to the measured peaks. Obviously, the measured spectra are richer than those predicted by the simplified model, and a complete explanation requires a more detailed description of the beam dynamics, such as the one based on the 3-dimensional strong-strong code. The results of the BeamBeam3D simulations are very similar to the data. The comparison between data (vertical) and simulations (both horizontal and vertical) suggests that the effect of coupling, not included in simulations, is non-negligible and may account for some of the discrepancies.

CONCLUSIONS

A system was developed to measure the spectra of coherent beam-beam oscillations of individual bunches in the Fermilab Tevatron collider. It is based on the analysis of the digitized signal from a single beam-position monitor. It requires applying band-limited noise to the beam, but an extension of its dynamic range is possible, if needed, so as to operate without excitation.

The device has a response time of a few seconds, a frequency resolution of 1.6×10^{-5} in fractional tune, and it is sensitive to oscillation amplitudes of 60 nm. In terms of sensitivity, resolution, and background level, it provides a very clean measurement of coherent oscillations in hadron machines. The system is complementary to Schottky detectors and transfer-function measurements as a diagnostic tool for tunes, tune spreads, and beam-beam effects. At the beginning of a collider store, when strong coherent lines distort the incoherent Schottky tune spectrum, the present system may provide a more accurate indication of betatron tunes.

Coherent oscillations in the Tevatron were stable, probably thanks to the different intensities of the two beams, their tune separation, and chromaticity. The average amplitude of the oscillations around the ring was estimated to be of the order of 20 nm. Patterns in the oscillation amplitude as a function of position along the bunch were observed. They may be related to the physical nature of the coherent modes. The phase of the oscillations as a function of frequency and bunch number may also provide physical insight, but it was not considered in this analysis.

A simplified collision model was used to calculate normal mode frequencies and to show their dependence on beam-beam coupling. Some scenarios were simulated using the self-consistent 3-dimensional strong-strong numerical code BeamBeam3D. Models were compared with observations made over the course of a collider store, as the strength of the beam-beam force decreased with time. Some discrepancies were observed, but the overall agreement was satisfactory considering the uncertainties on the antiproton parameters, such as lattice tunes and coupling, and their variation over time.

ACKNOWLEDGMENTS

The authors would like to thank V. Kamerdzhiev (Forschungszentrum Jülich, Germany), F. Emanov (Budker Institute for Nuclear Physics, Novosibirsk, Russia), Y. Alexahin, B. Fellenz, V. Lebedev, G. Saewert, V. Scarpine, A. Semenov, and V. Shiltsev (Fermilab) for their help and insights.

Fermi Research Alliance, LLC operates Fermilab under Contract No. DE-AC02-07-CH-11359 with the United States Department of Energy (US DOE). Brookhaven National Laboratory is operated by Brookhaven Science Associates, LLC under Contract No. DE-AC02-98-CH-10886 with the US DOE. This work was partially supported by the US LHC Accelerator Research Program (LARP).

REFERENCES

[1] A. Piwinski, IEEE Trans. Nucl. Sci. **26**, 4268 (1979).

[2] T. Ieiri, T. Kawamoto, and K. Hirata, Nucl. Instrum. Methods Phys. Res. A **265**, 364 (1988).

[3] E. Keil, K. Cornelis, and K. Hirata, in Proceedings of the 15th International Conference on High Energy Accelerators, Hamburg, Germany, p. 1106 (1992).

[4] I. N. Nesterenko, E. A. Perevedentsev, and A. A. Valishev, Phys. Rev. E **65**, 056502 (2002).

[5] J. P. Koutchouk, CERN Report No. ISR-OP/JPK-svw (19 March 1982).

[6] J. P. Koutchouk, CERN Report No. ISR-OP/JPK-bm (15 June 1982).

[7] W. Fischer et al., BNL Report No. C-AD/AP/75 (2002).

[8] W. Fischer et al., in Proceedings of the 2003 Particle Accelerator Conference (PAC03), Portland, Oregon, USA, 12–16 May 2003, p. 135.

[9] T. Pieloni, Ph.D. thesis, École Polytechnique Fédérale de Lausanne, Switzerland (2008).

[10] G. Stancari and A. Valishev, Phys. Rev. ST Accel. Beams **15**, 041002 (2012).

[11] X. Buffat et al., in Proceedings of the 2011 International Particle Accelerator Conference (IPAC11), San Sebastián, Spain, 4–9 September 2011, p. 1870.

[12] Y. Alexahin, Part. Accel. **59**, 43 (1998).

[13] V .Shiltsev et al., Phys. Rev. ST Accel. Beams **2**, 071001 (1999).

[14] V. Shiltsev et al., New J. Phys. **10**, 043042 (2008).

[15] V. Shiltsev et al., Phys. Rev. ST Accel. Beams **11**, 103501 (2008).

[16] A. Valishev and G. Stancari, in Proceedings of the 2011 Particle Accelerator Conference (PAC11), New York, New York, USA, 28 March – 1 April 2011, p. 67.

[17] R. E. Meller and R. H. Siemann, IEEE Trans. Nucl. Sci. **28**, 2431 (1981).

[18] K. Yokoya and H. Koiso, Part. Accel. **27**, 181 (1990).

[19] W. Herr, M. P. Zorzano, and F. Jones, Phys. Rev. ST Accel. Beams **4**, 054402 (2001).

[20] Y. Alexahin, Nucl. Instrum. Methods Phys. Res. A **480**, 253 (2002).

[21] T. Pieloni and W. Herr, in Proceedings of the 2005 Particle Accelerator Conference (PAC05), Knoxville, Tennessee, USA, 16–20 May 2005, p. 4030.

[22] J. Qiang et al., Phys. Rev. ST Accel. Beams **5**, 104402 (2002).

[23] J. Qiang et al., Nucl. Instrum. Methods Phys. Res. A **558**, 351 (2006).

[24] E. G. Stern et al., Phys. Rev. ST Accel. Beams **13**, 024401 (2010).

[25] J.-P. Carneiro et al., Fermilab Report No. Beams-doc-1911-v1 (unpublished).

[26] A. Semenov et al., in Proceedings of the 2007 Particle Accelerator Conference (PAC07), Albuquerque, New Mexico, USA, 25–29 June 2007, p. 3877.

[27] V. Kamerdzhiev, V. Lebedev, and A. Semenov, in Proceedings of the 2008 Beam Instrumentation Workshop (BIW08), Tahoe City, California, 4–8 May 2008, p. 300.

[28] A. Valishev et al., in Proceedings of the 2008 European Particle Accelerator Conference (EPAC08), Genoa, Italy, 23–27 June 2008, p. 3158.

[29] G. Stancari, A. Valishev, and A. Semenov, in Proceedings of the 2010 Beam Instrumentation Workshop (BIW10), Santa Fe, New Mexico, USA, 2–6 May 2010, p. 363.

[30] K. Yokoya, Phys. Rev. ST Accel. Beams **3**, 124401 (2000).

[31] R Development Core Team, *R: A language and environment for statistical computing* (R Foundation for Statistical Computing, Vienna, Austria, 2010), ISBN 3-900051-07-0.

[32] B. Baklakov et al., in Proceedings of the 1999 Particle Accelerator Conference (PAC99), New York, New York, USA, 29 March – 2 April 1999, p. 1387.

[33] V. Shiltsev, G. Stancari, and A. Valishev, J. Instrum. **6**, P08002 (2011).

[34] W. H. Press et al., *Numerical Recipes: The Art of Scientific Computing* (Cambridge University Press, 3rd ed., 2007).